

# <sup>1</sup> QhX: A Python package for periodicity detection in red noise

<sup>3</sup> **Andjelka B. Kovačević**  <sup>1\*</sup>, **Dragana Ilić**  <sup>1</sup>, **Momčilo Tošić** <sup>1\*</sup>, **Marina**  
<sup>4</sup> **Pavlović**  <sup>2</sup>, **Aman Raju**  <sup>1</sup>, **Mladen Nikolić**  <sup>1</sup>, **Saša Simić**  <sup>3</sup>, **Iva Čvorović**  
<sup>5</sup> **Hajdinjak**  <sup>1</sup>, and **Luka Č. Popović**  <sup>4</sup>

<sup>6</sup> **1** University of Belgrade-Faculty of Mathematics, Studentski trg 16, Belgrade, Serbia **2** Mathematical  
<sup>7</sup> Institute of Serbian Academy of Science and Arts, Serbia **3** Faculty of sciences, University of Kragujevac,  
<sup>8</sup> Radoja Domanovića 12, Serbia **4** Astronomical Observatory, Belgrade, Serbia  Corresponding author \*  
<sup>9</sup> These authors contributed equally.

DOI: [10.xxxxxx/draft](https://doi.org/10.xxxxxx/draft)

## Software

- [▪ Review](#) 
- [▪ Repository](#) 
- [▪ Archive](#) 

Editor: [Open Journals](#) 

## Reviewers:

- [▪ @openjournals](#)

Submitted: 01 January 1970

Published: unpublished

## License

Authors of papers retain copyright and release the work under a Creative Commons Attribution 4.0 International License ([CC BY 4.0](#)).

## <sup>10</sup> Summary

<sup>11</sup> QhX is a Python package for detecting periodicity in red noise time series, developed as an  
<sup>12</sup> in-kind contribution to the Vera C. Rubin Observatory Legacy Survey of Space and Time  
<sup>13</sup> (LSST, [Ivezić et al., 2019](#)). Traditional Fourier-based methods often struggle with red noise,  
<sup>14</sup> which is common in quasar light curves and other accreting objects. QhX addresses these  
<sup>15</sup> challenges with its core 2D Hybrid method ([Kovačević et al., 2018](#)). Input data are mapped  
<sup>16</sup> into a time-period plane via wavelet transforms, which are (auto)correlated to produce a  
<sup>17</sup> correlation density map in a “period-period” plane. Statistical vetting incorporates significance,  
<sup>18</sup> upper and lower error bounds, and the novel Intersection over Union (IoU) metric to evaluate  
<sup>19</sup> the proximity and overlap of detected periods across bands and objects. In addition to a vetted  
<sup>20</sup> numerical catalog, QhX dynamically visualizes periodicity across photometric bands and objects.

<sup>21</sup> **Statement of need**

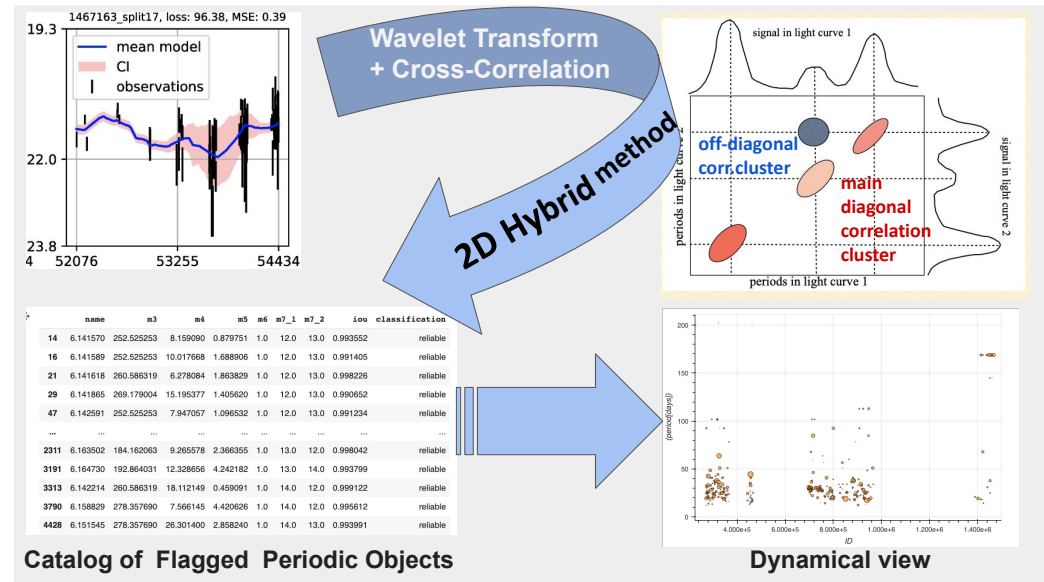
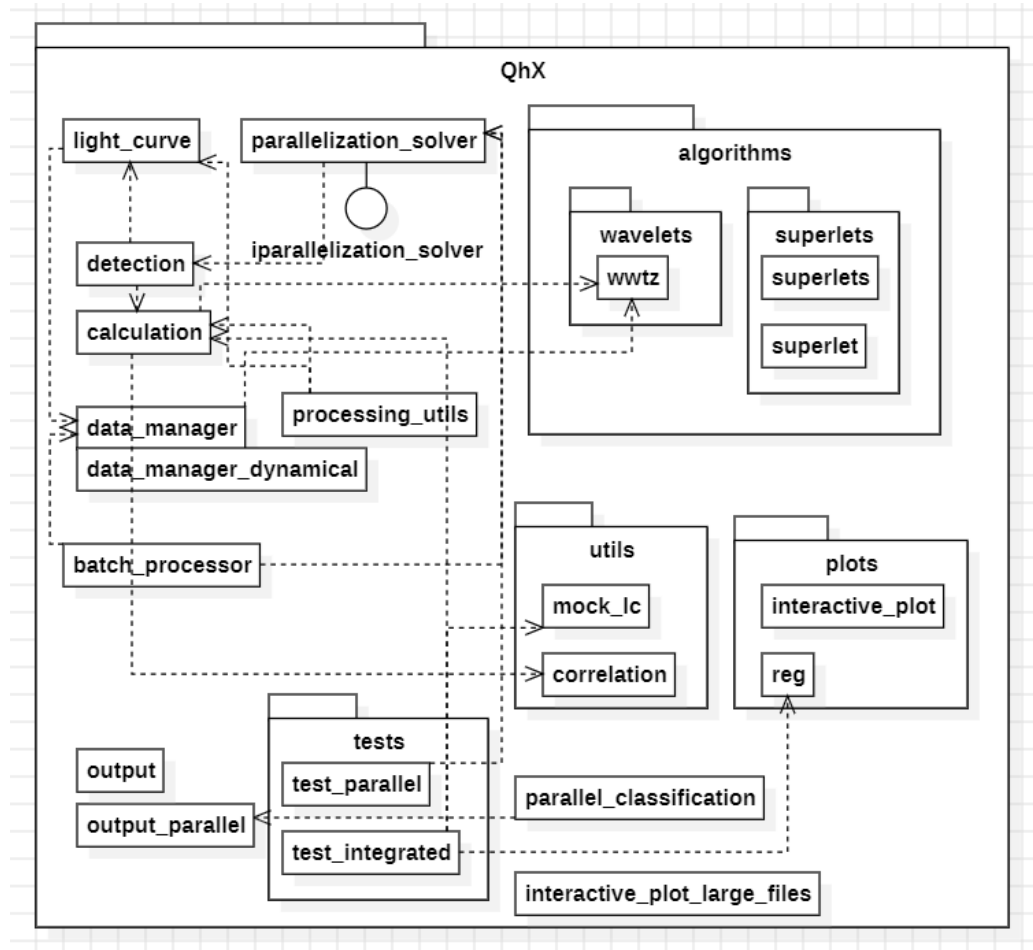


**Figure 1:** The left panel shows a 1D light curve with observational data (black error bars) and a model (blue line). QhX transforms the time-series into the time-frequency domain and cross-correlates wavelet matrices to produce a 2D period-period correlation map (right), where clusters indicate periodic signals. After map integration, statistical vetting generates a numerical catalog of flagged periodic objects (bottom left) and a dynamic view of detected periods across objects and bands (bottom right).

<sup>22</sup> Periodic variability spans a range of astronomical objects, from asteroids to quasars. Identifying  
<sup>23</sup> meaningful signals is complicated by red noise (see, e.g., Figure 1 in [Gaia Collaboration et al., 2019](#);  
<sup>24</sup> [Kasliwal et al., 2015](#); [Kovačević, Radović, et al., 2022](#)), which exhibits fractal-like  
<sup>25</sup> patterns across time scales ([Belete et al., 2018](#); [Vio et al., 1991](#)). Non-stationary signals and  
<sup>26</sup> unfavorable sampling ([Brandt et al., 2018](#); [D’Orazio & Charisi, 2023](#)) further obscure coherent  
<sup>27</sup> patterns. Traditional time-frequency methods, constrained by the Fourier uncertainty principle  
<sup>28</sup> (i.e., Gabor limit, [Gabor, 1947](#)), often fail with such complex signals, highlighting the need for  
<sup>29</sup> nonlinear approaches ([Abry et al., 1995](#); [Cohen, 1995](#)).

<sup>30</sup> QhX provides features specifically designed to address these challenges. The first feature is its  
<sup>31</sup> core 2D Hybrid method (see Figure 1), detailed in ([Kovačević et al., 2018](#)), inspired by 2D  
<sup>32</sup> Correlation Spectroscopy ([Kovačević, 2024](#); [Noda, 2018](#)). By applying wavelet transforms, QhX  
<sup>33</sup> maps time-series data into the time-frequency domain and (auto)correlates it, generating a  
<sup>34</sup> period-period correlation density that enhances signal detection. Secondly, QhX introduces an  
<sup>35</sup> Intersection over Union (IoU) metric, combined with standard statistical measures (significance,  
<sup>36</sup> upper and lower error bounds), to evaluate the overlap of detected periods across bands and  
<sup>37</sup> objects. Each period is represented as the center of an “IoU ball,” with its radius reflecting  
<sup>38</sup> relative error, calculated as the mean of the upper and lower error bounds—analogous to a  
<sup>39</sup> circular aperture in photometry ([Saxena et al., 2024](#)). Thirdly, QhX enhances traditional analysis  
<sup>40</sup> by generating numerical and interactive visual catalogs that rank periodicity candidates by  
<sup>41</sup> reliability. These interactive catalogs enable detailed inspection of signal consistency, offering  
<sup>42</sup> greater interpretability than traditional static plots.

## 43 QhX structure



44 Figure 2: Schematic representation of the QhX package architecture.

45 QhX (Version 0.2.0) is an open-source package optimized for gappy quasar light curves but  
 46 adaptable to other datasets. It supports both dynamic and fixed modes, with parallel processing  
 47 capabilities for large-scale data. The modular design facilitates rapid experimentation by  
 48 enabling easy swapping or modification of functions (see Figure 2), addressing diverse research  
 49 needs. For fixed-only workflows, specialized functions such as `data_manager` offer minimal  
 50 overhead and optimal performance, while `data_manager_dynamical` supports both dynamic  
 and fixed configurations to handle more complex scenarios involving dynamic filters.

51 The package is organized as follows:

- 52 1. **Core:**
  - 53     ▪ algorithms module provides essential signal-processing techniques, including the  
 54         Weighted Wavelet Z-Transform (`wwtz`) and prototype superlet transforms.
  - 55     ▪ correlation function within the `utils` module supports the 2D Hybrid method by  
 56         converting light curve data into wavelet matrices and performing (auto)correlation,  
 57         creating correlation density.
- 58 2. **Signal Detection and Validation:**
  - 59     ▪ detection module identifies candidate periodic signals and assesses their validity  
 60         using statistical measures (significance and upper and lower error (Johnson et al.,  
 61         2019)). The Intersection over Union (IoU) metric identifies overlapping periods

62 across bands and objects. To our knowledge, this is the first application of the  
63 Intersection-over-Union (IoU) metric to quantify the overlap between detected and  
64 reference periods in astronomical time-series analysis.

- 65 ▪ Statistical vetting categorizes detected periods for each object and band as reliable,  
66 medium, or poor.

67 **3. Data Management:**

- 68 ▪ QhX assumes input time-series data in a simple tabular format containing time,  
69 flux (or magnitude), and associated uncertainties. Examples in the documentation  
70 illustrate how to map data from other commonly used formats into this structure.
- 71 ▪ `data_manager` and `data_manager_dynamical` modules manage data flow, data  
72 loading, outlier removal, and format compatibility.
- 73 ▪ `batch_processor` and `parallelization_solver` modules optimize task distribution  
74 across multiple processors.

75 **4. Visualization and Output:**

- 76 ▪ `plots` module includes tools for creating interactive visualizations, such as  
77 `interactive_plot`, which allows for exploring detected periodicities across bands  
78 and objects. For large datasets, `interactive_plot_large_files` enables in-depth  
79 inspection of signal consistency.
- 80 ▪ `output` and `output_parallel` modules handle result storage, supporting both  
81 single-threaded and parallelized workflows.

82 **5. Testing:**

- 83 ▪ `tests` module, containing `test_parallel` and `test_integrated`, validates the  
84 functionality across various processing setups.

## 85 Representative Applications

86 QhX has been benchmarked with respect to widely used periodicity detection software across  
87 multiple domains. In Fatović et al. (2023), applying QhX to SDSS J2320 $\pm$ \$0024 yielded a  
88 period of  $278.36_{-25.21}^{+57.34}$  days, with a significance above 99% measured via the shuffling method,  
89 and a 90% significance from the Generalized Extreme Value (GEV) approach. A Lomb–Scargle  
90 periodogram applied to the same dataset produced a consistent period of 278~days at the  
91 same significance level. In Kovačević et al. (2019), QhX detected periods of  $1972 \pm 254$ ~days  
92 (observed light curve) and  $1873 \pm 250$  days (modeled light curve) for PG~1302–102, both  
93 within  $1\sigma$  of the  $1884 \pm 88$  day period reported by Graham et al. (2015) using generalized  
94 Lomb–Scargle, wavelet, and autocorrelation methods; a Bayesian reanalysis by Zhu & Thrane  
95 (2020) on an extended dataset for PG~1302–102 yielded a comparable quasi-period of 5.6  
96 yr, interpreted as quasiperiodic oscillations. In the case of Mrk 231 (Kovačević, Yi, et al.,  
97 2020), the 2D hybrid method identified a characteristic period of 403 days with a significance  
98 greater than 99.7%, in agreement with a Lomb–Scargle periodogram result of 413 days at  
99 a significance above 95%; the slightly larger uncertainty in the QhX-derived period reflects  
100 the temporal variation of the periodicity, while the average oscillation power is comparable  
101 between the two methods. The method has also been validated in the context of damped  
102 oscillations in the changing-look quasar NGC 3516 (Kovačević, Popović, et al., 2020), where  
103 experimental results demonstrated robustness against the combined effects of red noise and  
104 complex time-series structure. Beyond astrophysical applications, QhX has been applied to  
105 Very Low Frequency (VLF) signal analysis for pre- and post-earthquake intervals (Kovačević,  
106 Nina, et al., 2022). In the no-earthquake scenario (same date one year earlier), the topology of  
107 QhX 2D hybrid maps exhibited distinct correlation cluster patterns compared to earthquake-day  
108 records, with detected periods below 111 s in most intervals and a  $\sim 140$  s signal in the  $\sim 2$  h  
109 segment, closely matching a 147 s signal detected during the earthquake event. Comparison  
110 with Fast Fourier Transform (FFT) results (Nina et al., 2020) showed strong agreement before  
111 the earthquake for periods below 1.5 min, and convergence of both methods to similar values  
112 in subsequent intervals. Post-earthquake periods obtained with QhX were also consistent with  
113 the  $< 10$ s to few-hundred-second range reported in (Ohya et al., 2018). QhX is the LSST

<sup>114</sup> directable software in-kind contribution.

## <sup>115</sup> Acknowledgements

<sup>116</sup> Funding was provided by the University of Belgrade - Faculty of Mathematics (the contract  
<sup>117</sup> 451-03-66/2024-03/200104), Faculty of Sciences University of Kragujevac (451-03-65/2024-  
<sup>118</sup> 03/200122), and Astronomical Observatory Belgrade (contract 451-03-66/2024- 03/200002),  
<sup>119</sup> through grants by the Ministry of Education, Science, and Technological Development of the  
<sup>120</sup> Republic of Serbia.

## <sup>121</sup> References

- <sup>122</sup> Abry, P., Gonçalvès, P., & Flandrin, P. (1995). *Wavelets, spectrum analysis and 1/f processes*  
<sup>123</sup> (A. Antoniadiis & G. Oppenheim, Eds.; pp. 15–29). Springer New York. [https://doi.org/10.1007/978-1-4612-2544-7\\_2](https://doi.org/10.1007/978-1-4612-2544-7_2)
- <sup>125</sup> Belete, A. B., Bravo, J. P., Canto Martins, B. L., Leão, I. C., De Araujo, J. M., & De  
<sup>126</sup> Medeiros, J. R. (2018). Multifractality signatures in quasars time series - I. 3C 273. 478(3),  
<sup>127</sup> 3976–3986. <https://doi.org/10.1093/mnras/sty1316>
- <sup>128</sup> Brandt, W. N., Ni, Q., Yang, G., Anderson, S. F., Assef, R. J., Barth, A. J., Bauer, F. E.,  
<sup>129</sup> Bongiorno, A., Chen, C.-T., De Cicco, D., Gezari, S., Grier, C. J., Hall, P. B., Hoenig,  
<sup>130</sup> S. F., Lacy, M., Li, J., Luo, B., Paolillo, M., Peterson, B. M., ... Yu, Z. (2018). Active  
<sup>131</sup> Galaxy Science in the LSST Deep-Drilling Fields: Footprints, Cadence Requirements, and  
<sup>132</sup> Total-Depth Requirements. *arXiv e-Prints*, arXiv:1811.06542. <https://doi.org/10.48550/arXiv.1811.06542>
- <sup>134</sup> Cohen, L. (1995). *Time-frequency analysis*. Prentice Hall PTR. ISBN: 9780135945322
- <sup>135</sup> D'Orazio, D. J., & Charisi, M. (2023). Observational Signatures of Supermassive Black Hole  
<sup>136</sup> Binaries. *arXiv e-Prints*, arXiv:2310.16896. <https://doi.org/10.48550/arXiv.2310.16896>
- <sup>137</sup> Fatović, M., Palaversa, L., Tisanić, K., Thanjavur, K., Ivezić, Ž., Kovačević, A. B., Ilić, D., &  
<sup>138</sup> Č. Popović, L. (2023). Detecting Long-period Variability in the SDSS Stripe 82 Standards  
<sup>139</sup> Catalog. 165(4), 138. <https://doi.org/10.3847/1538-3881/acb596>
- <sup>140</sup> Gabor, D. (1947). Acoustical quanta and the theory of hearing. *Nature*, 159(4044), 591–594.  
<sup>141</sup> <https://doi.org/10.1038/159591a0>
- <sup>142</sup> Gaia Collaboration, Eyer, L., Rimoldini, L., Audard, M., Anderson, R. I., Nienartowicz, K.,  
<sup>143</sup> Glass, F., Marchal, O., Grenon, M., Mowlavi, N., Holl, B., Clementini, G., Aerts, C., Mazeh,  
<sup>144</sup> T., Evans, D. W., Szabados, L., Brown, A. G. A., Vallenari, A., Prusti, T., ... Zwitter, T.  
<sup>145</sup> (2019). Gaia Data Release 2. Variable stars in the colour-absolute magnitude diagram.  
<sup>146</sup> *Astronomy & Astrophysics*, 623, A110. <https://doi.org/10.1051/0004-6361/201833304>
- <sup>147</sup> Graham, M. J., Djorgovski, S. G., Stern, D., Glikman, E., Drake, A. J., Mahabal, A. A., Donalek,  
<sup>148</sup> C., Larson, S., & Christensen, E. (2015). A possible close supermassive black-hole binary in  
<sup>149</sup> a quasar with optical periodicity. 518(7537), 74–76. <https://doi.org/10.1038/nature14143>
- <sup>150</sup> Ivezić, Ž., Kahn, S. M., Tyson, J. A., Abel, B., Acosta, E., Allsman, R., Alonso, D., AlSayyad,  
<sup>151</sup> Y., Anderson, S. F., Andrew, J., Angel, J. R. P., Angeli, G. Z., Ansari, R., Antilogus, P.,  
<sup>152</sup> Araujo, C., Armstrong, R., Arndt, K. T., Astier, P., Aubourg, É., ... Zhan, H. (2019). LSST:  
<sup>153</sup> From Science Drivers to Reference Design and Anticipated Data Products. 873(2), 111.  
<sup>154</sup> <https://doi.org/10.3847/1538-4357/ab042c>
- <sup>155</sup> Johnson, M. A. C., Gandhi, P., Chapman, A. P., Moreau, L., Charles, P. A., Clarkson, W.  
<sup>156</sup> I., & Hill, A. B. (2019). Prospecting for periods with LSST - low-mass X-ray binaries  
<sup>157</sup> as a test case. *Monthly Notices of the Royal Astronomical Society*, 484(1), 19–30.

- 158        <https://doi.org/10.1093/mnras/sty3466>
- 159        Kasliwal, V. P., Vogeley, M. S., & Richards, G. T. (2015). Are the variability properties of the  
160        Kepler AGN light curves consistent with a damped random walk? *Monthly Notices of the  
161        Royal Astronomical Society*, 451(4), 4328–4345. <https://doi.org/10.1093/mnras/stv1230>
- 162        Kovačević, A. B. (2024). Two-dimensional (2D) hybrid method: Expanding 2D corre-  
163        lation spectroscopy (2D-COS) for time series analysis. *Applied Spectroscopy*, 0(0),  
164        00037028241241308. <https://doi.org/10.1177/00037028241241308>
- 165        Kovačević, A. B., Nina, A., Popović, L. Č., & Radovanović, M. (2022). Two-dimensional  
166        correlation analysis of periodicity in noisy series: Case of VLF signal amplitude variations  
167        in the time vicinity of an earthquake. *Mathematics*, 10(22). <https://doi.org/10.3390/math10224278>
- 169        Kovačević, A. B., Pérez-Hernández, E., Popović, L. Č., Shapovalova, A. I., Kollatschny, W., &  
170        Ilić, D. (2018). Oscillatory patterns in the light curves of five long-term monitored type 1  
171        active galactic nuclei. 475(2), 2051–2066. <https://doi.org/10.1093/mnras/stx3137>
- 172        Kovačević, A. B., Popović, L. Č., & Ilić, D. (2020). Two-dimensional correlation analysis of  
173        periodicity in active galactic nuclei time series. *Open Astronomy*, 29(1), 51–55. <https://doi.org/10.1515/astro-2020-0007>
- 175        Kovačević, A. B., Popović, L. Č., Simić, S., & Ilić, D. (2019). The Optical Variability of  
176        Supermassive Black Hole Binary Candidate PG 1302-102: Periodicity and Perturbation in  
177        the Light Curve. 871(1), 32. <https://doi.org/10.3847/1538-4357/aaf731>
- 178        Kovačević, A. B., Radović, V., Ilić, D., Popović, L. Č., Assef, R. J., Sánchez-Sáez, P., Nikutta,  
179        R., Raiteri, C. M., Yoon, I., Homayouni, Y., Li, Y.-R., Caplar, N., Czerny, B., Panda, S.,  
180        Ricci, C., Jankov, I., Landt, H., Wolf, C., Kovačević-Dojčinović, J., ... Marčeta-Mandić, S.  
181        (2022). The LSST Era of Supermassive Black Hole Accretion Disk Reverberation Mapping.  
182        262(2), 49. <https://doi.org/10.3847/1538-4365/ac88ce>
- 183        Kovačević, A. B., Yi, T., Dai, X., Yang, X., Čvorović-Hajdinjak, I., & Popović, L. Č. (2020).  
184        Confirmed short periodic variability of subparsec supermassive binary black hole candidate  
185        Mrk 231. 494(3), 4069–4076. <https://doi.org/10.1093/mnras/staa737>
- 186        Nina, A., Pulinets, S., Biagi, P. F., Nico, G., Mitrović, S. T., Radovanović, M., & Popović, L.  
187        Č. (2020). Variation in natural short-period ionospheric noise, and acoustic and gravity  
188        waves revealed by the amplitude analysis of a VLF radio signal on the occasion of the  
189        kraljevo earthquake (mw= 5.4). *Science of the Total Environment*, 710, 136406.
- 190        Noda, I. (2018). Chapter 2 - advances in two-dimensional correlation spectroscopy (2DCOS).  
191        In J. Laane (Ed.), *Frontiers and advances in molecular spectroscopy* (pp. 47–75). Elsevier.  
192        <https://doi.org/https://doi.org/10.1016/B978-0-12-811220-5.00002-2>
- 193        Ohya, H., Tsuchiya, F., Takishita, Y., Shinagawa, H., Nozaki, K., & Shiokawa, K. (2018).  
194        Periodic oscillations in the d region ionosphere after the 2011 tohoku earthquake using LF  
195        standard radio waves. *Journal of Geophysical Research: Space Physics*, 123(6), 5261–5270.
- 196        Saxena, A., Salvato, M., Roster, W., Shirley, R., Buchner, J., Wolf, J., Kohl, C., Starck, H.,  
197        Dwelly, T., Comparat, J., & al., et. (2024). CIRCLEZ : Reliable photometric redshifts for  
198        active galactic nuclei computed solely using photometry from Legacy Survey Imaging for  
199        DESI. 690, A365. <https://doi.org/10.1051/0004-6361/202450886>
- 200        Vio, R., Cristiani, S., Lessi, O., & Salvadori, L. (1991). 3C 345: Is the Variability of Quasars  
201        Nonlinear? 380, 351. <https://doi.org/10.1086/170594>
- 202        Zhu, X.-J., & Thrane, E. (2020). Toward the Unambiguous Identification of Supermassive  
203        Binary Black Holes through Bayesian Inference. 900(2), 117. <https://doi.org/10.3847/1538-4357/abac5a>